Research Article Vol. 4, No. 8 / 15 August 2021 / OSA Continuum 2133

High spectral purity microwave generation using a dual-frequency hybrid integrated semiconductor-dielectric waveguide laser

JESSE MAK,[1,*] ALBERT VAN REES,[1] ROB E. M. LAMMERINK,[1] DIMITRI GESKUS,[2] YOUWEN FAN,[1] PETER J. M. VAN DER SLOT,[1] CHRIS G. H. ROELOFFZEN,[2] AND KLAUS-J. BOLLER[1,3]

[1]*Laser Physics and Nonlinear Optics Group, MESA+ Institute for Nanotechnology, Department of Science and Technology, University of Twente, Enschede, The Netherlands*
[2]*LioniX International BV, Enschede, The Netherlands*
[3]*Optical Technologies Group, Institute of Applied Physics, University of Münster, Münster, Germany*
[*]*j.mak@utwente.nl*

Abstract: We present an integrated semiconductor-dielectric hybrid dual-frequency laser operating in the 1.5 μm wavelength range for microwave and terahertz (THz) generation. Generating a microwave beat frequency near 11 GHz, we observe an intrinsic linewidth as low as about 2 kHz. This is realized by hybrid integration of a single diode amplifier based on indium phosphide (InP) with a long, low-loss silicon nitride (Si_3N_4) feedback circuit to extend the cavity photon lifetime, resulting in a cavity optical roundtrip length of about 30 cm on a chip. Simultaneous lasing at two frequencies is enabled by introducing an external control parameter for balancing the feedback from two tunable, frequency-selective Vernier mirrors on the Si_3N_4 chip. Each frequency can be tuned with a wavelength coverage of about 80 nm, potentially allowing for the generation of a broad range of frequencies in the microwave range up to the THz range.

1. Introduction

Photonic integrated microwave sources exhibiting low phase noise are of strong interest for applications such as microwave photonics [1], time and frequency metrology [2], and coherent radar sensing [3]. There are various promising methods to photonically generate microwaves, e.g., via mode-locked lasers [4], Kerr frequency combs [5], and opto-electronic oscillators (OEOs) [6]. However, a disadvantage with mode-locking and Kerr combs is the limited tunability of the generated frequency, which is fixed by the cavity roundtrip length. An attractive alternative, which we exploit here, is to realize a narrow-linewidth dual-frequency laser to generate a beat note at the difference frequency. This approach enables the generation of a wide range of frequencies in the microwave range up to the terahertz (THz) range via tuning of the two laser lines.

For most applications it is important to reduce the slow noise, i.e., close-to-carrier phase noise, also called technical noise. However, reducing the intrinsic linewidth (also termed fast noise, Lorentzian linewidth component, fundamental linewidth, or Schawlow-Townes linewidth [7]) is still of high importance for applications involving fast timescales, such as wireless communication in the microwave and THz range [8,9]. For example, wireless links employing advanced modulation formats, such as QAM [10], benefit from low intrinsic linewidths via reduced bit error rates [11]. In addition, working with low intrinsic linewidth is advantageous for locking of oscillators with phase locked loops, avoiding the need for high loop bandwidths [12]. Here our focus is to realize a dual-frequency laser with a narrow intrinsic linewidth, for fast applications and as preparation for active stabilization.

#424586 https://doi.org/10.1364/OSAC.424586
Journal © 2021 Received 29 Mar 2021; revised 28 Jun 2021; accepted 7 Jul 2021; published 22 Jul 2021

OSA CONTINUUM

Bulk dual-frequency fiber lasers [13] and solid state lasers [14] for microwave generation have been demonstrated. Aiming on chip-scale sources, dual-wavelength rare-earth-doped waveguide lasers have been widely explored as well [15], but these lasers require optical pumping, which introduces additional complexity. It is therefore attractive to use semiconductor lasers, which are directly pumped by an electric current. Semiconductor dual-wavelength lasers have been studied in the form of distributed feedback (DFB) lasers with a single gain section and a partly shared cavity [16], and as distributed Bragg reflector (DBR) lasers with separate gain sections and separate laser cavities combined with a Y-junction [17].

The main problem of all on-chip dual-frequency semiconductor lasers realized so far is that the intrinsic linewidth of the individual laser frequencies is broad, e.g., around 60 MHz in [16], essentially due to a short cavity photon lifetime in combination with high gain-index coupling [18]. A well-known solution is to increase the photon lifetime by increasing the cavity length using low-loss waveguides. In this direction, there have been studies on heterogeneous integrated III-V/silicon dual-frequency lasers [19,20]. In [19], a single laser cavity is used to generate a beat frequency at 0.357 THz with a 3 dB linewidth of 4.2 MHz retrieved via a wider-span Lorentzian fit. In [20], two separate laser cavities and a photodetector are integrated on the same chip and used to generate beat frequencies between 1 and 112 GHz. The individual lasers showed 3 dB linewidths of 148 kHz, retrieved with narrower-span Lorentzian fits. Monolithic InP extended cavity lasers were used to generate beat frequencies with narrow 3 dB linewidths of 250 kHz [21] and 56 kHz [22] based on wider-span Lorentzian fits. A narrow intrinsic microwave linewidth of 39.5 kHz [23], retrieved from the power spectral density of instantaneous frequency far from carrier (2 - 100 MHz), was realized using a dual-frequency hybrid integrated laser based on silicon waveguides. The narrowest linewidth value reported so far for an all-chip based electrically driven dual-frequency laser is 26 kHz (3 dB linewidth obtained from a smoothed beat signal) using a monolithic InAs/InP quantum dash dual-frequency laser with a common cavity [24]. However, in all these approaches the photon lifetime, and thus the intrinsic linewidth, is ultimately limited by the use of semiconductor waveguides, which have relatively high linear and nonlinear loss [25,26].

Here, we take an important step beyond such limits by extending the cavity photon lifetime using a low-loss dielectric feedback circuit via hybrid integration. Specifically, we use an indium phosphide (InP) amplifier hybrid integrated with a long and low-loss silicon nitride (Si_3N_4) feedback circuit (Fig. 1), which extends the optical roundtrip length of the solitary amplifier from about 0.5 cm to 30 cm, i.e., by a large factor of about 60. To enable dual-frequency lasing, we introduce a tunable coupler which directs the light towards two frequency-selective loop mirrors that can be controlled independently. These mirrors are based on tunable microring resonators in Vernier configuration, as this allows also for wide wavelength coverage in single-frequency operation and enables continuous (mode-hop free) tunability over a wide range [27]. We use the dual-frequency laser to generate narrow linewidth microwave radiation at a frequency near 11 GHz, and observe a narrow intrinsic linewidth of around 2 kHz.

We note that generating continuous-wave narrow intrinsic linewidth radiation is promising with quantum cascade lasers (QCLs) as well, but their room temperature operation as desired is restricted so far to much higher frequencies in the far-infrared region above 10 THz and the mid-IR region [28]. An alternative solution to access also the THz region at room temperature is found in intra-cavity difference frequency generation [29].

Closest to our study is the recent demonstration of two lasers using two separate semiconductor optical amplifiers of different materials (InP and GaAs) that are hybrid integrated with separate feedback circuits on the same dielectric (Si_3N_4) chip [30]. The aim of that study was to generate light in two largely different wavelength ranges (1.5 and 1 μm), with the future goal of generating mid-IR radiation via difference frequency generation. The individual lasers had relatively low 3 dB linewidths of 18 and 70 kHz retrieved with a lower-span Lorentzian fit.

OSA CONTINUUM

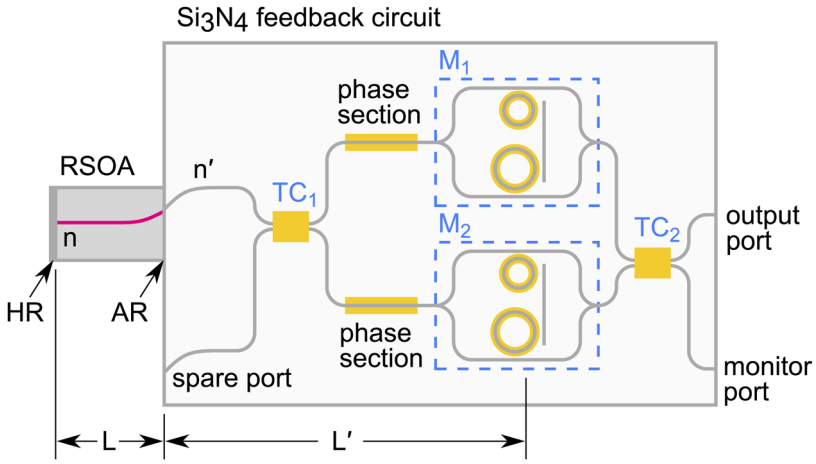

Fig. 1. Schematic diagram of the dual-frequency hybrid laser (not to scale). The reflective semiconductor optical amplifier (RSOA) is equipped on one facet with a high-reflection (HR) coating, and on the other facet with an anti-reflection (AR) coating. The silicon nitride (Si_3N_4) feedback chip contains two tunable couplers (labeled TC_1 and TC_2), two phase sections, and two Vernier mirrors (labeled M_1 and M_2) providing frequency-selective feedback. Each Vernier mirror consists of two microring resonators (MRRs), which have slightly different ring radii $R_1 = 125$ μm and $R_2 = 127.5$ μm. The tunable couplers, phase sections, and ring resonators can be tuned using resistive electric heaters, indicated in yellow.

In contrast to that study and other previous work [20], we generate the two frequencies from a single gain medium, because this can enable additional linewidth reduction, as was demonstrated before [13,16,23]. The motivation is that the frequency fluctuation of the two modes may experience some synchronization if they are initiated by a common cause. However, providing dual-frequency lasing with a single gain medium is also difficult with semiconductor lasers. First, lasers using advanced semiconductor quantum well gain media typically suffer from strong gain competition due to homogeneous broadening of the gain, which makes it difficult to establish simultaneous oscillation at two frequencies. Single-gain dual-frequency operation therefore requires an additional control parameter that balances the relative feedback. Second, noise correlation effects at fast noise frequencies are more complex for semiconductors because of the following effects. On the one hand, one expects that the two laser modes undergo independent phase excursions due to independent spontaneous emission noise. On the other hand, as quantified by Henry's linewidth enhancement factor, most of the intrinsic linewidth is due to index fluctuations associated with fluctuations in population inversion [18], which should still be seen by both oscillating frequencies. In hybrid and heterogeneously integrated lasers with spectrally narrow feedback filtering, additional effects influence the intrinsic linewidth, specifically an all-optical feedback loop based on the coupling between feedback strength and index, which is usually expressed as the linewidth reduction factor B [31–33].

Here, we present the first dual-frequency, hybrid integrated diode laser with low-loss feedback based on Si_3N_4 waveguide circuits and a single gain medium. Although synchronized frequency fluctuations seem present only in part of the spectra, we achieve a low intrinsic linewidth of the microwave beat of these frequencies of about 2 kHz, measured at around 11 GHz. We note that a much lower linewidth was achieved for microwave generation with Brillouin oscillators at discrete frequencies, optically pumped with an external laser [34]. In comparison, our intrinsic linewidth value is, to our best knowledge, a record for fully chip-based dual-frequency lasers that are electrically pumped and widely tunable. Thereby, this work demonstrates novel options for

OSA CONTINUUM

on-chip high spectral purity microwave generation and, due to wide and independent tunability of the output frequencies, also for THz generation. With further extension of the cavity length, these lasers are of promise for further linewidth reduction as can be seen from recent measurements at single frequencies [33,35].

2. Methods

A schematic diagram of the dual-frequency laser is shown in Fig. 1. The laser consists of a double-pass reflective semiconductor optical amplifier (RSOA) chip, which generates light at a wavelength around 1.55 μm, and silicon nitride (Si_3N_4 in SiO_2) chip, which extends the cavity length and provides frequency-selective feedback for dual-frequency lasing. The RSOA chip [36], fabricated by the Fraunhofer Heinrich Hertz Institute, contains an InP-based multi-quantum well active waveguide with a length of $L = 700$ μm and a group index of $n = 3.6$. One facet is equipped with a high-reflection (HR) coating (reflectance 90%) and forms one of the cavity mirrors. To minimize back reflections into the guided mode of the RSOA, the other facet (at the Si_3N_4-InP interface) is equipped with an anti-reflection (AR) coating. In addition, near the interface the amplifier waveguide is angled with respect to the facet normal by 9 degrees.

The Si_3N_4 feedback circuit is, in contrast to previously reported hybrid lasers [27,35,37], fabricated with an asymmetric double stripe (ADS) cross section. Compared to symmetric double stripe (SDS) waveguides, these require less fabrication steps and offer similar propagation loss [38]. The ADS Si_3N_4 waveguides have a group index (n') of 1.77. For optimum coupling efficiency, near the interface, the Si_3N_4 waveguide is tilted by about 20 degrees with respect to the facet normal. Two-dimensional tapering [38] was used for optimized matching to the mode field of the RSOA.

To enable lasing at two frequencies, which we refer to as f_1 and f_2, the circuit contains two Vernier loop mirrors (M_1 and M_2). To provide a total Vernier free spectral range ($\Delta\lambda_{FSR,tot}$) in the order of the gain bandwidth [39], these loop mirrors contain two microring resonators (MRRs) which have slightly different radii ($R_1 = 125$ μm, $R_2 = 127.5$ μm; $\Delta\lambda_{FSR,tot} = 87$ nm). The power coupling to the bus waveguides was designed to be 1%, to realize significant cavity length enhancement at resonance (enhancement factor $F = 99$), due to multiple passes through the MRRs [40]. In total, the effective optical roundtrip length of the hybrid laser cavity is about 30 cm, i.e., a factor of about 60 longer than the roundtrip length of the solitary amplifier ($2nL \approx 0.5$ cm).

To enable dual-frequency oscillation despite the presence of gain competition, we have incorporated a Mach-Zehnder interferometer (MZI) based tunable coupler (labeled TC_1) to balance the feedback levels from M_1 and M_2. We note that the tunability of the feedback balance during laser operation is an important control parameter that also allows to investigate a possible influence of shared index fluctuations in the RSOA on the linewidth of the microwave frequency. To combine the laser output behind both Vernier mirrors into a single output port, the signals are superimposed using another tunable coupler (TC_2).

All MRRs are equipped with thermo-electric heaters to enable tuning of the Vernier peaks, which makes it possible to set the laser to different light frequencies, f_1 and f_2. To set f_1, for example, to a desired value close to f_2, we simultaneously tune the two MRRs belonging to M_1 at the correct ratio, given by the ratio of MRR lengths. This ratio was experimentally found to be 1.03 for both M_1 and M_2. We recall that continuous mode-hop free tuning of a single-frequency version of the laser was demonstrated to span a range of 28 GHz [27]. This suggests that with a dual-frequency laser, mode-hop free tuning of the beat frequency over a range of 56 GHz would be possible.

The RSOA chip and Si_3N_4 chip are hybridly integrated, and permanently fixed to a mount that is kept at a constant temperature (25 °C) using a Peltier cooler. The RSOA current and heater voltages are provided using in-house built USB-controlled printed circuit boards. To characterize

OSA CONTINUUM

the dual-frequency laser, the output is guided through an optical isolator to a 50:50 fiber splitter. 50 percent of the output power is guided to an optical spectrum analyzer (OSA; Ando AQ6317, spectral resolution 0.01 nm). To generate and inspect beat notes directly in the microwave domain, the remaining light is guided to a fast photodetector (Discovery Semiconductors DSC30S, 20 GHz bandwidth) connected to an electrical spectrum analyzer (ESA; Agilent E4405B).

3. Results

Without adjusting TC_1 to balance the feedback levels of the two Vernier mirrors, the hybrid laser generally shows single-frequency oscillation due to spectral condensation. The laser output power is about 1.5 mW at a pump current of 100 mA. The highest output power we observed was 5.5 mW using a pump current of 200.6 mA. With synchronized heating of the MRRs as described above, each wavelength can be independently controlled with a spectral coverage of 80 nm, which is close to the gain bandwidth of the diode.

Dual-frequency operation is achieved by balancing the feedback levels of the Vernier mirrors using TC_1. Figure 2(a) shows a typical example of the dual-frequency laser spectrum (OSA resolution 125 GHz), where the two frequencies (f_1 and f_2) are tuned to a frequency difference of 1.5 THz (12 nm). For microwave generation which can be easily measured using the photodiode and ESA, the laser lines are tuned close to each other, here to a distance of 11 GHz (0.09 nm). The optical spectrum is shown in Fig. 2(b). The figure displays a wider overview of the spectrum at low resolution (125 GHz) and a narrower window at higher resolution (1.25 GHz) in the inset, where the two laser lines can be distinguished, as well as two higher order sidebands. To demonstrate narrow-linewidth microwave generation, we guided the dual-frequency output to a fast photodetector and recorded the electrical spectrum, which is shown in Fig. 3(a). The spectrum displays a sharp peak near 11 GHz, which matches the frequency difference in the optical spectrum (Fig. 2(b)). To inspect the intrinsic linewidth, we recorded multiple microwave spectra using a narrower frequency window (50 MHz). The center frequency and spectral shape showed some variation over time due to remaining technical noise, e.g., from acoustic fluctuations or noise in the pump current. To avoid developing an active stabilization for removal of slower

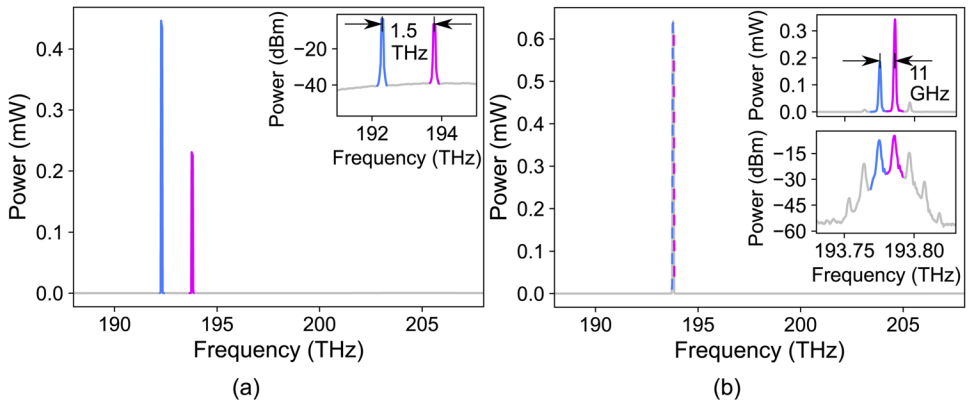

Fig. 2. Measured dual-frequency optical spectra with the two laser lines (highlighted in blue and pink) tuned to a frequency difference of (a) 1.5 THz (12 nm), and (b) 11 GHz (0.09 nm). Both (a) and (b) provide a wider overview at lower resolution (125 GHz). The inset of (a) displays the same spectrum on a logarithmic scale, which shows that the side mode suppression ratios of the two laser lines with regard to the broadband background are at least 35 dB and 30 dB, respectively. The insets of (b) show a narrower frequency window with higher resolution (1.25 GHz), where the two laser lines can be seen. The bottom inset is plotted logarithmically and shows higher order sidebands.

OSA CONTINUUM

variations, we characterized the free-running laser with repeated recordings of sufficiently short acquisition time (4 ms).

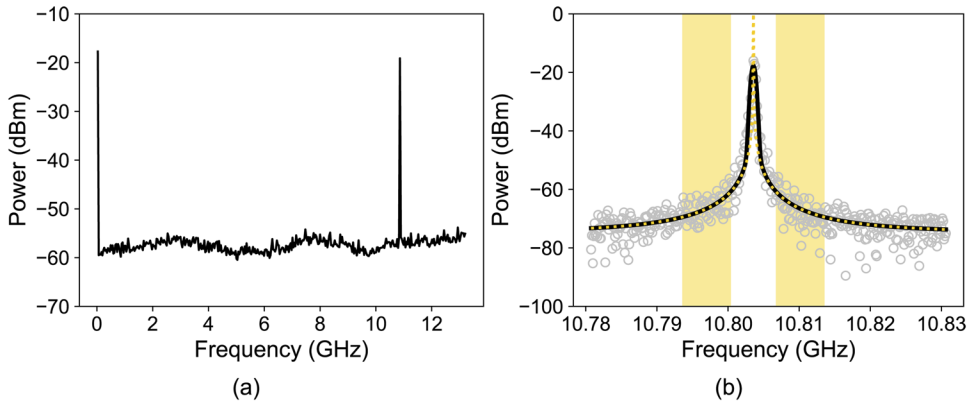

Fig. 3. (a) Beat frequency near 11 GHz, measured using a fast photodetector and an electrical spectrum analyzer (ESA) set to a resolution and video bandwidth of 3 MHz each. (b) Example of the beat frequency (open circles) measured using a narrower frequency window (50 MHz), with a resolution and video bandwidth of 300 kHz each. The solid line represents a Voigt fit with a Gaussian (technical noise) component w_G = 0.42 MHz and a Lorentzian component w_L = 5.4 kHz (FWHM). Here, w_G was a free fit parameter, while w_L was kept fixed and was determined by fitting a Lorentzian (yellow dashed line). The fit is based only on data in the center of the wings (shaded areas), which reduces biasing by non-Lorentzian components from the Gaussian line center and flat noise floor.

Figure 3(b) shows a representative example of the generated microwave spectra. The spectrum follows a Voigt profile (solid line in Fig. 3(b)), with a Gaussian-shaped center indicating technical noise, and Lorentzian-shaped wings due to the intrinsic optical linewidths of the laser. To determine the intrinsic linewidth of the microwave spectra, we applied a Lorentzian least-square fit (dashed yellow line) to the center of the wings, which reduces biasing by the Gaussian-shaped line center and the flat noise floor. The Lorentzian width of the spectra, which sets the intrinsic linewidth, showed some variation over time. This is likely caused by a residual drift of the light frequencies with regard to the center frequencies of the Vernier filters. Such drift can reduce the number of roundtrips in the MRRs, thereby shortening also the laser's effective cavity length. To provide information not only on the narrowest linewidth that can be achieved, we performed longer-term linewidth recording, i.e., we performed 80 recordings of the beat note in sequence, without realignment, with an interval of a few seconds between each acquisition.

Figure 4(a) shows the intrinsic linewidth values (FWHM) that we obtained for the 80 spectra. The error bars represent the 95% confidence intervals calculated from the standard error in the fitted linewidth. Figure 4(b) shows the same data as a histogram. The horizontal dashed lines in Figs. 4(a) and (b) indicate the minimum, median, and maximum linewidths. To provide an indication of the typical linewidth value, we chose to present the median value rather than the average, because the average (5.7 kHz) is slightly skewed by a small number of larger linewidth values. The broadest linewidth that we observed is 23 ± 4 kHz. The median linewidth value is 4.2 kHz. The lowest observable linewidth was 1.8 ± 0.3 kHz, which is, to our best knowledge, the narrowest intrinsic linewidth obtained so far for microwave generation using free-running, chip-integrated, electronically pumped, and widely tunable dual-frequency lasers.

To pursue also the question whether generating the two frequencies from a single gain section allows for microwave linewidths narrower than the convolution of the individual laser frequencies, we measured also the intrinsic linewidth of the individual laser frequencies. As we

OSA CONTINUUM

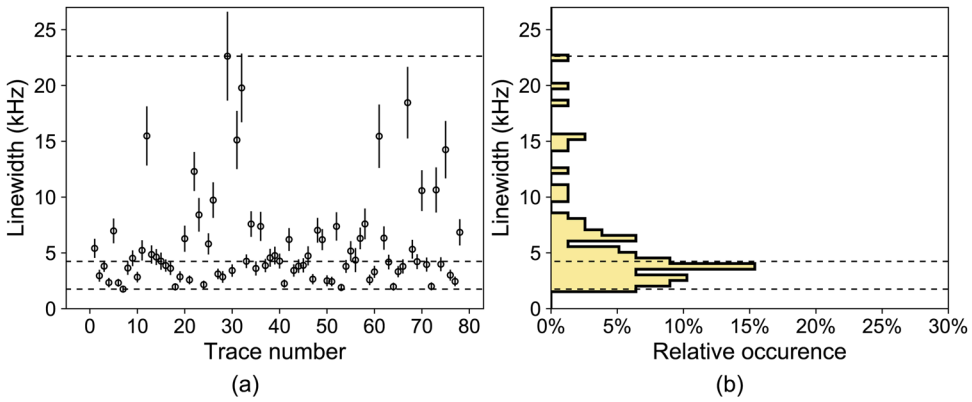

Fig. 4. (a) Intrinsic linewidths of the generated 11-GHz microwave signal obtained with longer term recording of the free-running dual-frequency laser output. The vertical error bars represent the 95% confidence intervals calculated from the standard error of the fit parameter. (b) Distribution of the measured linewidth values. The horizontal dashed lines indicate the minimum, median, and maximum linewidth values.

are investigating intrinsic linewidth components of Lorentzian shape, this convolution can be expressed by adding the optical linewidths.

To enable measuring the individual optical linewidths, with f_1 and f_2 set to the same distance of about 11 GHz, we temporarily imbalanced TC_1 until the spectrum collapsed to a single frequency, first at f_1 and then at f_2, and adjusted the phase section for narrowest linewidth. We measured the intrinsic linewidth via delayed self-heterodyne detection [41] using the experimental setup described in [35] with 20 km fiber delay, resulting in a spectral resolution of about 10 kHz. Again we record multiple spectra and for each spectrum fit a Lorentzian far from the line center and noise floor. We note that this measurement is not limited by the spectral resolution. Using a 50 MHz window, and a 300 kHz resolution and video bandwidth, we found the linewidth distributions shown in Figs. 5(a) and (b). As indicated by the dashed lines, the measurements yielded two somewhat different median linewidth values for the two laser frequencies, namely 1.9 kHz (at f_1) and 5.4 kHz (at f_2). This may be addressed to the two Vernier feedback circuits providing a somewhat different extension of the cavity length, which enters the intrinsic linewidth approximately quadratically [42]. This difference is likely caused in the f_2-feedback circuit by one MRR resonance being slightly detuned with respect to the other MRR resonance, which reduces the number of roundtrips through the MRRs. The same trend of a narrower linewidth with the f_1-feedback circuit was found in all measurements. The minimum individual linewidths that were observable are as low as 0.4 ± 0.1 kHz (at f_1) and 1.7 ± 0.2 kHz (at f_2).

To interpret the optical linewidth data in context of the measured microwave linewidths, we recall that if correlations in the frequency fluctuations of the two laser lines are absent, the microwave linewidth should be given by the sum of the two individual Lorentzian linewidths. Looking at the median individual linewidths, one would then expect a microwave linewidth of $1.9 + 5.4 = 7.3$ kHz. However, the measured median microwave linewidth (4.2 kHz) is clearly smaller than 7.3 kHz. This observation suggests that the two laser lines show correlated frequency fluctuations. However, when comparing the minimum linewidth values, the microwave linewidth (1.8 ± 0.3 kHz) is, within the experimental error, the same as the added individual linewidths (2.1 ± 0.3 kHz). A possible explanation is that the minimum linewidth values occurred for near-optimum alignment of the light frequencies with respect to the Vernier center frequencies, i.e., slightly detuned, which leads to compensation of inversion induced index and frequency fluctuations, expressed via the linewidth reduction factor B [31–33]. As the linewidth data

OSA CONTINUUM

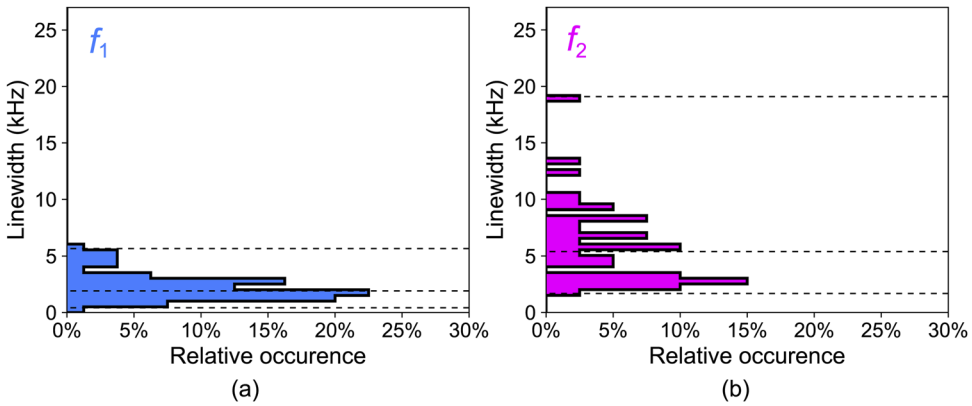

Fig. 5. Distribution of the measured intrinsic linewidths for (a) the laser line at f_1, and (b) the laser line at f_2, each after collapse to single-frequency oscillation. The linewidths were obtained from self-heterodyne beat spectra recorded using an electrical spectrum analyzer (ESA). The minimum, median, and maximum linewidth values are indicated by the horizontal dashed lines.

presented so far do not provide sufficient evidence of synchronized noise in the two tones, further experimental exploration is certainly required. An option would be to employ a highly dispersive fiber and measure whether the beat linewidth increases with fiber length, which would give a proof of synchronized frequency fluctuations. Generally, recording the spectral density of phase noise or frequency noise would provide more information than available so far. Although further research is certainly required, it appears that we have found traces of a beneficial correlation in the fast frequency fluctuations of a dual-frequency diode laser caused by the use of a single gain element.

4. Summary and conclusion

In summary, we have presented a hybrid integrated dual-frequency laser for microwave and THz generation. With the example of microwave generation at 11 GHz, we observe extremely low intrinsic linewidths with a median value of 4.2 kHz in measurement series and 1.8 ± 0.3 kHz (smallest linewidth). These values are, to our knowledge, the narrowest linewidths reported so far for microwaves generated by a free-running, fully chip-integrated, electrically driven, and widely tunable dual-frequency laser. This is achieved by hybrid integrating a single InP amplifier with a low-loss dielectric (Si_3N_4) feedback circuit, which extends the optical roundtrip length by a large factor of about 60 with respect to the solitary diode, i.e., from about 0.5 cm to 30 cm on a chip, and provides feedback for dual-frequency lasing via two independently tunable, frequency-selective Vernier mirrors.

Our approach can provide tunable microwave and THz generation at a wide range of frequencies, from low frequencies in the RF or microwave range up to 10 THz, because the InP-Si_3N_4 lasers that were used here have a large spectral coverage, essentially covering the entire gain bandwidth [27]. The narrow linewidth we have demonstrated should also be found back in the THz range when applying the appropriate linewidth analysis [43]. In addition, mode-hop free tunability in the microwave and THz regime could be implemented straightforwardly via synchronous tuning of the microring resonators and phase sections as was demonstrated recently with a similar, single-frequency InP-Si_3N_4 hybrid integrated laser [27]. The Si_3N_4 platform used in our approach enables attractive options for microwave photonics, as it enables co-integration with advanced components such as modulators and filters [1].

OSA CONTINUUM

Future studies should focus on further clarification and possibly exploitation of correlations in the frequency noise of dual-frequency diode lasers with hybrid integrated feedback from low-loss dielectric waveguide circuits, for further linewidth narrowing in the microwave and THz range. We note that even if such noise correlation turns out to be limited, there lies significant potential for further linewidth narrowing by using longer feedback circuits [35], potentially resulting in microwave and THz linewidths below the 100 Hz level.

Funding. Nederlandse Organisatie voor Wetenschappelijk Onderzoek (13537); H2020 LEIT Information and Communication Technologies (3PEAT,780502); Rijksdienst voor Ondernemend Nederland (IPD12009).

Acknowledgments. We thank C. A. A. Franken, H. M. J. Bastiaens, and D. Marpaung for support and suggestions.

Disclosures. The authors declare no conflicts of interest.

Data availability. Data underlying the results presented in this paper are not publicly available at this time but may be obtained from the authors upon reasonable request.

References

1. D. Marpaung, J. Yao, and J. Capmany, "Integrated microwave photonics," Nat. Photonics **13**(2), 80–90 (2019).
2. J. Millo, M. Abgrall, M. Lours, E. M. L. English, H. Jiang, J. Guéna, A. Clairon, M. E. Tobar, S. Bize, Y. Le Coq, and G. Santarelli, "Ultralow noise microwave generation with fiber-based optical frequency comb and application to atomic fountain clock," Appl. Phys. Lett. **94**(14), 141105 (2009).
3. P. Ghelfi, F. Laghezza, F. Scotti, G. Serafino, A. Capria, S. Pinna, D. Onori, C. Porzi, M. Scaffardi, A. Malacarne, V. Vercesi, E. Lazzeri, F. Berizzi, and A. Bogoni, "A fully photonics-based coherent radar system," Nature **507**(7492), 341–345 (2014).
4. M.-C. Lo, R. Guzmán, and G. Carpintero, "InP femtosecond mode-locked laser in a compound feedback cavity with a switchable repetition rate," Opt. Lett. **43**(3), 507–510 (2018).
5. W. Liang, D. Eliyahu, V. S. Ilchenko, A. A. Savchenkov, A. B. Matsko, D. Seidel, and L. Maleki, "High spectral purity Kerr frequency comb radio frequency photonic oscillator," Nat. Commun. **6**(1), 7957 (2015).
6. L. Maleki, "Sources: The optoelectronic oscillator," Nat. Photonics **5**(12), 728–730 (2011).
7. A. L. Schawlow and C. H. Townes, "Infrared and optical masers," Phys. Rev. **112**(6), 1940–1949 (1958).
8. G. Carpintero, K. Balakier, Z. Yang, R. C. Guzmán, A. Corradi, A. Jimenez, G. Kervella, M. J. Fice, M. Lamponi, M. Chitoui, F. van Dijk, C. C. Renaud, A. Wonfor, E. A. J. M. Bente, R. V. Penty, I. H. White, and A. J. Seeds, "Microwave photonic integrated circuits for millimeter-wave wireless communications," J. Lightwave Technol. **32**(20), 3495–3501 (2014).
9. A. J. Seeds, H. Shams, M. J. Fice, and C. C. Renaud, "TeraHertz photonics for wireless communications," J. Lightwave Technol. **33**(3), 579–587 (2015).
10. P. J. Winzer and R.-J. Essiambre, "Advanced optical modulation formats," Proc. IEEE **94**(5), 952–985 (2006).
11. H. Shams, L. Gonzalez-Guerrero, M. Fice, Z. Yang, C. Renaud, and A. Seeds, "Distribution of multiband THz wireless signals over fiber," Proc. SPIE **10128**, 101280G (2017).
12. K. Balakier, L. Ponnampalam, M. J. Fice, C. C. Renaud, and A. J. Seeds, "Integrated semiconductor laser optical phase lock loops," IEEE J. Sel. Top. Quantum Electron. **24**(1), 1–12 (2018).
13. X. Chen, Z. Deng, and J. Yao, "Photonic generation of microwave signal using a dual-wavelength single-longitudinal-mode fiber ring laser," IEEE Trans. Microwave Theory Tech. **54**(2), 804–809 (2006).
14. M. Alouini, M. Brunel, F. Bretenaker, M. Vallet, and A. Le Floch, "Dual tunable wavelength Er:Yb:glass laser for terahertz beat frequency generation," IEEE Photonics Technol. Lett. **10**(11), 1554–1556 (1998).
15. C. Grivas, "Optically pumped planar waveguide lasers: Part II: Gain media, laser systems, and applications," Prog. Quantum Electron. **45-46**, 3–160 (2016).
16. F. Pozzi, R. M. De La Rue, and M. Sorel, "Dual-wavelength InAlGaAs-InP laterally coupled distributed feedback laser," IEEE Photonics Technol. Lett. **18**(24), 2563–2565 (2006).
17. R. K. Price, V. B. Verma, K. E. Tobin, V. C. Elarde, and J. J. Coleman, "Y-branch surface-etched distributed Bragg reflector lasers at 850 nm for optical heterodyning," IEEE Photonics Technol. Lett. **19**(20), 1610–1612 (2007).
18. C. Henry, "Theory of the linewidth of semiconductor lasers," IEEE J. Quantum Electron. **18**(2), 259–264 (1982).
19. H. Shao, S. Keyvaninia, M. Vanwolleghem, G. Ducournau, X. Jiang, G. Morthier, J.-F. Lampin, and G. Roelkens, "Heterogeneously integrated III-V/silicon dual-mode distributed feedback laser array for terahertz generation," Opt. Lett. **39**(22), 6403–6406 (2014).
20. J. Hulme, M. J. Kennedy, R.-L. Chao, L. Liang, T. Komljenovic, J.-W. Shi, B. Szafraniec, D. Baney, and J. E. Bowers, "Fully integrated microwave frequency synthesizer on heterogeneous silicon-III/V," Opt. Express **25**(3), 2422–2431 (2017).
21. G. Carpintero, E. Rouvalis, K. Ławniczuk, M. Fice, C. C. Renaud, X. J. M. Leijtens, E. A. J. M. Bente, M. Chitoui, F. van Dijk, and A. J. Seeds, "95 GHz millimeter wave signal generation using an arrayed waveguide grating dual wavelength semiconductor laser," Opt. Lett. **37**(17), 3657–3659 (2012).
22. R. C. Guzmán, A. Jimenez, V. Corral, G. Carpintero, X. J. M. Leijtens, and K. Ławniczuk, "Narrow linewidth dual-wavelength laser sources based on AWG for the generation of millimeter wave signals," in *XXIX Simposium*

OSA CONTINUUM

Nacional de la Unión Científica Internacional de Radio, A. G. Salvador, ed. (Universitat Politècnica de València, 2014).
23. X. Huang, C. R. Doerr, C. Qin, J. Heanue, N. Zhu, D. Ton, B. Guan, S. Zhang, and Y. Zhao, "Silicon-photonic laser emitting tunable dual wavelengths with highly correlated phase noise," Opt. Lett. **46**(1), 142–145 (2021).
24. M. Rahim, K. Zeb, Z. Lu, G. Pakulski, J. Liu, P. Poole, C. Song, P. Barrios, W. Jiang, and X. Zhang, "Monolithic InAs/InP quantum dash dual-wavelength DFB laser with ultra-low noise common cavity modes for millimeter-wave applications," Opt. Express **27**(24), 35368–35375 (2019).
25. M. J. R. Heck, J. F. Bauters, M. L. Davenport, D. T. Spencer, and J. E. Bowers, "Ultra-low loss waveguide platform and its integration with silicon photonics," Laser Photonics Rev. **8**(5), 667–686 (2014).
26. C. Xiang, W. Jin, J. Guo, C. Williams, A. M. Netherton, L. Chang, P. A. Morton, and J. E. Bowers, "Effects of nonlinear loss in high-Q Si ring resonators for narrow-linewidth III-V/Si heterogeneously integrated tunable lasers," Opt. Express **28**(14), 19926–19936 (2020).
27. A. van Rees, Y. Fan, D. Geskus, E. J. Klein, R. M. Oldenbeuving, P. J. M. van der Slot, and K.-J. Boller, "Ring resonator enhanced mode-hop-free wavelength tuning of an integrated extended-cavity laser," Opt. Express **28**(4), 5669–5683 (2020).
28. M. S. Vitiello, G. Scalari, B. Williams, and P. De Natale, "Quantum cascade lasers: 20 years of challenges," Opt. Express **23**(4), 5167–5182 (2015).
29. L. Consolino, S. Jung, A. Campa, M. De Regis, S. Pal, J. H. Kim, K. Fujita, A. Ito, M. Hitaka, S. Bartalini, P. De Natale, M. A. Belkin, and M. S. Vitiello, "Spectral purity and tunability of terahertz quantum cascade laser sources based on intracavity difference-frequency generation," Sci. Adv. **3**(9), e1603317 (2017).
30. Y. Zhu and L. Zhu, "Narrow-linewidth, tunable external cavity dual-band diode lasers through InP/GaAs-Si_3N_4 hybrid integration," Opt. Express **27**(3), 2354–2362 (2019).
31. K. Vahala and A. Yariv, "Detuned loading in coupled cavity semiconductor lasers — Effect on quantum noise and dynamics," Appl. Phys. Lett. **45**(5), 501–503 (1984).
32. T. Komljenovic, L. Liang, R.-L. Chao, J. Hulme, S. Srinivasan, M. Davenport, and J. E. Bowers, "Widely-tunable ring-resonator semiconductor lasers," Appl. Sci. **7**(7), 732 (2017).
33. M. A. Tran, D. Huang, J. Guo, T. Komljenovic, P. A. Morton, and J. E. Bowers, "Ring-resonator based widely-tunable narrow-linewidth Si/InP integrated lasers," IEEE J. Sel. Top. Quantum Electron. **26**(2), 1–14 (2020).
34. J. Li, H. Lee, and K. J. Vahala, "Microwave synthesizer using an on-chip Brillouin oscillator," Nat. Commun. **4**(1), 2097 (2013).
35. Y. Fan, A. van Rees, P. J. M. van der Slot, J. Mak, R. M. Oldenbeuving, M. Hoekman, D. Geskus, C. G. H. Roeloffzen, and K.-J. Boller, "Hybrid integrated InP-Si_3N_4 diode laser with a 40-Hz intrinsic linewidth," Opt. Express **28**(15), 21713–21728 (2020).
36. D. de Felipe, Z. Zhang, W. Brinker, M. Kleinert, A. M. Novo, C. Zawadzki, M. Moehrle, and N. Keil, "Polymer-based external cavity lasers: Tuning efficiency, reliability, and polarization diversity," IEEE Photonics Technol. Lett. **26**(14), 1391–1394 (2014).
37. J. Mak, A. van Rees, Y. Fan, E. J. Klein, D. Geskus, P. J. M. van der Slot, and K.-J. Boller, "Linewidth narrowing via low-loss dielectric waveguide feedback circuits in hybrid integrated frequency comb lasers," Opt. Express **27**(9), 13307–13318 (2019).
38. C. G. H. Roeloffzen, M. Hoekman, E. J. Klein, L. S. Wevers, R. B. Timens, D. Marchenko, D. Geskus, R. Dekker, A. Alippi, R. Grootjans, A. van Rees, R. M. Oldenbeuving, J. P. Epping, R. G. Heideman, K. Wörhoff, A. Leinse, D. Geuzebroek, E. Schreuder, P. W. L. van Dijk, I. Visscher, C. Taddei, Y. Fan, C. Taballione, Y. Liu, D. Marpaung, L. Zhuang, M. Benelajla, and K.-J. Boller, "Low-loss Si_3N_4 TriPleX optical waveguides: Technology and applications overview," IEEE J. Sel. Top. Quantum Electron. **24**(4), 1–21 (2018).
39. R. M. Oldenbeuving, E. J. Klein, H. L. Offerhaus, C. J. Lee, H. Song, and K.-J. Boller, "25 kHz narrow spectral bandwidth of a wavelength tunable diode laser with a short waveguide-based external cavity," Laser Phys. Lett. **10**(1), 015804 (2013).
40. B. Liu, A. Shakouri, and J. E. Bowers, "Passive microring-resonator-coupled lasers," Appl. Phys. Lett. **79**(22), 3561–3563 (2001).
41. T. Okoshi, K. Kikuchi, and A. Nakayama, "Novel method for high resolution measurement of laser output spectrum," Electron. Lett. **16**(16), 630–631 (1980).
42. M. W. Fleming and A. Mooradian, "Spectral characteristics of external-cavity controlled semiconductor lasers," IEEE J. Quantum Electron. **17**(1), 44–59 (1981).
43. G. Ducournau, P. Szriftgiser, T. Akalin, A. Beck, D. Bacquet, E. Peytavit, and J. F. Lampin, "Highly coherent terahertz wave generation with a dual-frequency Brillouin fiber laser and a 1.55 μm photomixer," Opt. Lett. **36**(11), 2044–2046 (2011).